The 2010 IEEE/RSJ International Conference on
Intelligent Robots and Systems
October 18-22, 2010, Taipei, Taiwan

Dynamical analysis and improvement of velocity for a 3 DOF precise inchworm mechanism

Ohmi Fuchiwaki and Kazushi Arafuka

Abstract— **In this paper, we describe the dynamical analysis and improvement of velocity for a precise inchworm mechanism with 3 DOF. This mechanism is composed of 4 piezoelectric actuators and pair of electromagnets and moves like an inchworm with less than a 10 nm resolution. We calculate the dynamical relationship between 3 DOF motion and 4 piezoelectric displacements. We also calculate the maximum velocity with no slip of electromagnets because the no slip condition is very important for motion repeatability. In several experiments, we have checked the theoretical validity and we confirm that the analysis procedure works well as an initial design of the inchworm mechanism. The design procedure, basic performance, and chip-mounting applications are also discussed as an advance in the new field of micro-robotics used in precision regions.**

I. INTRODUCTION

Recently, miniaturization of portable devices and electronic parts has been remarkable. Moving stages inside conventional chip-mounting devices are more than 100kg and big vibrations occur to the precise instruments around them, although electronic chip parts themselves are less than 1mg. The final goal of this study is the development of low-vibration, low-power and low-floorage mounting devices supported by 3 DOF precise inchworm mechanisms. In the last ten years, we have developed a unique inchworm mechanism composed of four piezoelectric actuators and two electromagnets. We have developed unique applications where these small mechanisms play important roles [1][2]. We show that small mobile mechanisms are effective in reducing the size and weight for precise instruments [3]–[6]. We also have developed a compensation and navigating device for this 3 DOF mechanism for accurate motion [7]. The main purpose of this paper is to study the maximum velocity with good motion repeatability to discuss applications of the mechanism. No slip of electromagnets is important in achieving good repeatability, however maximum velocity is also important in improving productive efficiency. To describe the maximum velocity, we analyze the relationships among the force and mass of electromagnets, displacements and spring constants of piezoelectric actuators by an approximate vibration model. We have also developed a new mechanism by using the analytical results to improve the maximum velocity. In several experiments, we confirm that we have increased maximum velocity over 2 times compared with conventional mechanisms. We also discuss an energy-efficient, cost-saving, and low-vibration chip mounting device organized by this tiny mobile mechanism to propose a new design for precise and flexible instruments.

Manuscript received March 10, 2010. Part of this study was supported by the "Promotion of Environmental Improvement for Independence of the Young Researchers" under the Special Coordination Funds for Promoting Science and Technology from the Ministry of Education, Culture, Sports, Science and Technology (MEXT) of Japan.

Ohmi Fuchiwaki is with the Interdisciplinary Research Center, Yokohama National University (YNU), 1-79 Tokiwadai, Hodogaya-ku, Yokohama, Kanagawa, Japan (phone: +81-45-339-3693; fax: +81-45-339-3693; e-mail: ohmif@ynu.ac.jp).

Kazushi Arafuka is with the Dept. of Mechanical Engineering, Yokohama National University (YNU)

II. STRUCTURE OF 3DOF INCHWORM MECHANISM

Fig.1 shows the structure of the precise miniature mechanism with 3 DOF. Two closed loop electromagnets, EM-1 and EM-2, arranged to cross each other are connected by four piezoelectric actuators, PZT-F, PZT-B, PZT-R, and PZT-L, so that the mechanism can move in any direction precisely in the manner of an inchworm. As shown in Fig.2, the mechanism can move in X and Y directions as well as rotate at a specified point precisely in the manner of an inchworm. This small mechanism can move flexibly and widely on the well-polished iron surface. Fig.3 shows the photographs of a conventional mechanism, "C" type. A joint mechanism composed of a V-shaped groove and a cylinder-shaped magnetic core is attached to one of 4 legs to stabilize simultaneously the contact of the 4 legs on the surface. Recently, we have developed a new type of the mechanism with a pair of amplified piezoelectric actuators

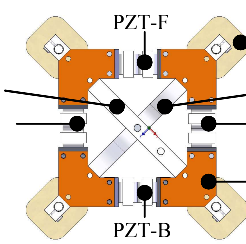

Fig. 1. Structure

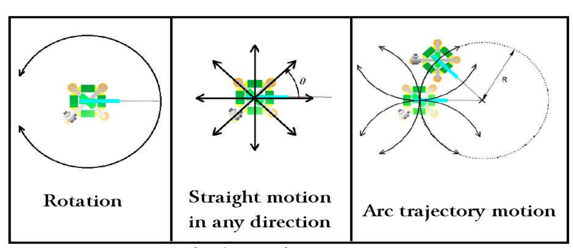

Fig. 2. Motion pattern

connected in a series to obtain larger step width as shown in Fig. 4. This new mechanism, the "G" type, also has parallel leaf springs for smooth contact of 4 legs on the surface. Table I shows a typical performance of the piezoelectric actuators. In this paper, we compare the performance of these 2 types, "C" and "G". Fig.5 shows the motion sequence. This mechanism moves like an inchworm while retaining the synchronism among rectangular-shaped forces of two electromagnets and sine-wave-shaped displacements of four piezoelectric actuators. Here A_F, A_B, A_R, and A_L are the displacement amplitudes. We define 1 step motion when the mechanism moves from t=0 to t=T. If we change the A_F, A_B, A_R, and A_L reasonably, the mechanism moves 3DOF precisely with less than a 10 nm resolution.

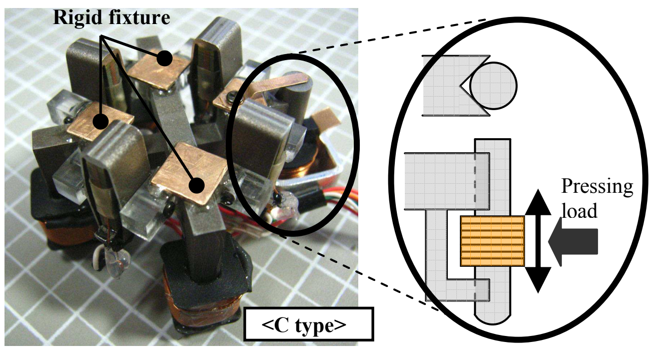

Fig. 3. Conventional mechanism with V-shaped groove and cylinder-shaped magnetic core

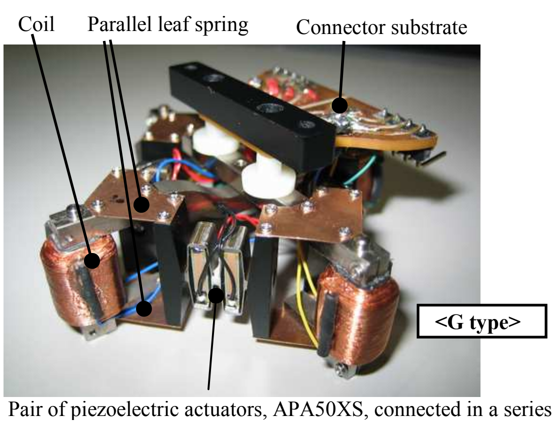

Fig. 4. Newly-developed mechanism with parallel leaf springs

TABLE I
PERFORMANCE OF PIEZOELECTRIC ACTUATORS

Quantity	APA35XS(C)	Pair of APA50XS(G)
Displacement (100V)	32.4 µm	100 µm
Generative Force (100V)	19.35 N	18 N
Spring constant	490,000 N/m	115,000 N/m
Capacitance	0.52 µF	0.26 µF
Natural Frequency (blocked free)	3.88 kHz	1.45 kHz
Height	12.85 mm	12.85 mm
Thickness	6.4 mm	6.4 mm
Length	4.6 mm	9.2 mm
Weight	2 g	4 g

III. Dynamical Analysis

A. Definition of dynamical model

As depicted in Fig. 6, we define the dynamical model of the

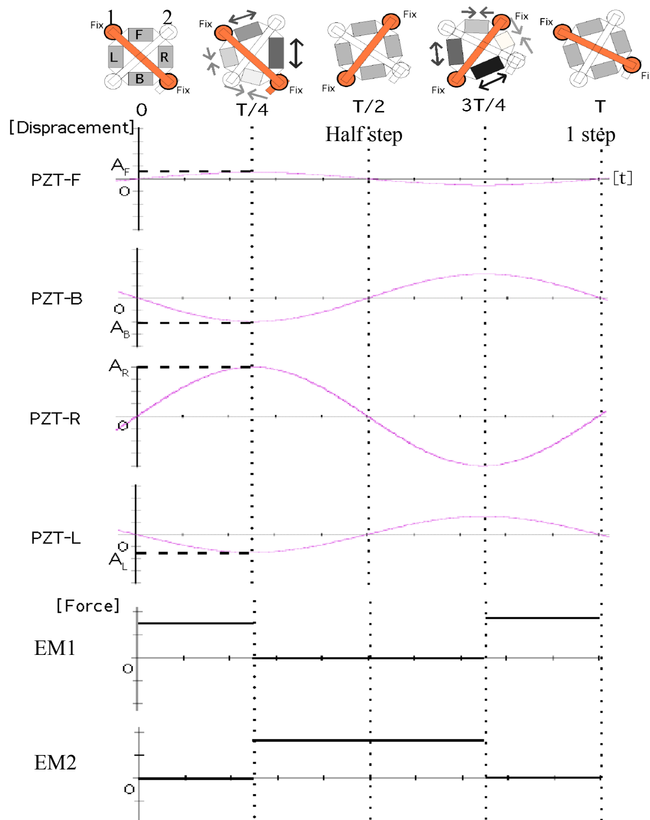

Fig. 5. Motion sequence of the inchworm locomotion

mechanism. Here, k_L is the spring constant of the piezoelectric actuators. d_F is the displacement of the piezoelectric actuator PZT_F. d_B, d_R and d_L are similarly defined. EM_1 and EM_2 are electromagnets separated from each other. We assume EM_1 and EM_2 are rigid bodies. P_1, P_2, P_3, and P_4 are hinged joints on EM_1 and EM_2. x_1 and y_1 are coordinates of P_1. x_2, y_2, x_3, y_3, x_4, and y_4 are similarly defined. P_{G1} is the gravity point of EM_1. P_{G2}, which is not shown in Fig. 6, is the gravity point of EM_2. The position of P_{G1} represents an orthogonal coordinate system used by x_{G1} and y_{G1}. O_{G1} and O_{G2} are the original points of P_{G1} and P_{G2} respectively. O_1, O_2, O_3, and O_4 are the initial positions of P_1, P_2, P_3, and P_4. We assume piezoelectric actuators move two electromagnets, EM_1 and EM_2. P_1, P_2, P_3, and P_4 are moved by four piezoelectric actuators. Displacements of EM_1 and EM_2 are determined by the positions of P_1, P_2, P_3, and P_4. We define the shearing force of PZT_F as F_{SF}. F_{SB}, F_{SR}, and F_{SL} are similarly defined. If k_S is the spring constant of the shear conversion of piezoelectric actuators, we can represent the shearing forces as follows:

$$F_{SF} = -k_s(y_1 - y_3)$$
$$F_{SB} = -k_s(y_2 - y_4)$$
$$F_{SR} = -k_s(x_1 - x_4)$$
$$F_{SL} = -k_s(x_2 - x_3)$$

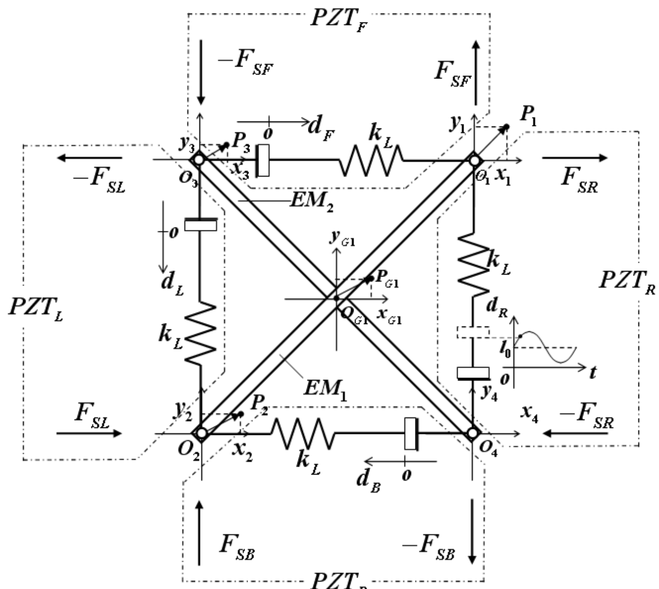

Fig. 6. Dynamical model of precise 3 DOF inchworm mechanism

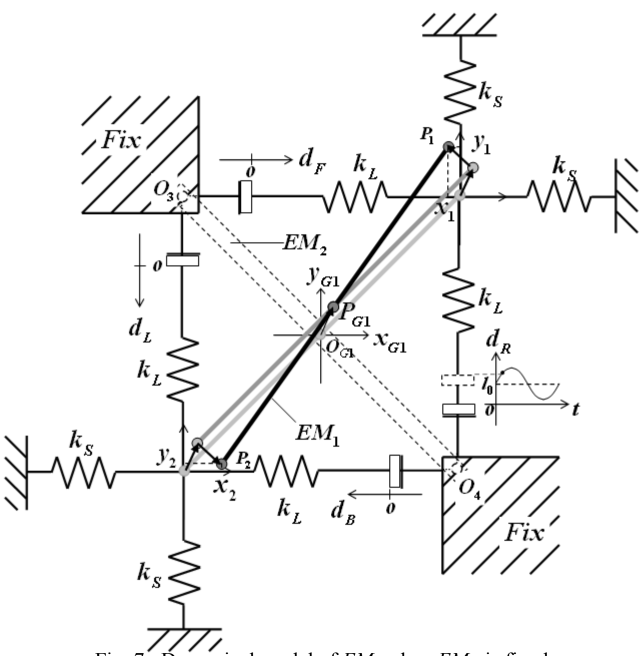

Fig. 7. Dynamical model of EM_1 when EM_2 is fixed

When EM_2 is fixed and EM_1 is free, we consider the 3 DOF dynamical model of EM_1 as depicted in Fig. 7. In this figure, we assume P_3 and P_4 are fixed at initial position O_3 and O_4 respectively. In this condition, x_3, y_3, x_4, and y_4 all become zero, so shearing forces become as follows:

$$F_{SF} = -k_s y_1$$

$$F_{SB} = -k_s y_2$$

$$F_{SR} = -k_s x_1$$

$$F_{SL} = -k_s x_2$$

We assume the residual deformation of PZT is negligible for the velocity, however it may influence the motion repeatability. We discuss the motion repeatability in another publication.

B. Calculation of dynamical model

Fig. 8 shows the vector resolution of the motion of EM_1. We represent the motion of the free magnet as a combination of translation and rotation. Here, $\vec{L}$ is the translational vector. $\vec{R}_1$ and $\vec{R}_2$ are rotational vectors. θ represents the rotational angle of EM_1. ϕ is direction of $\vec{L}$. We describe the triangle $P_{G1}P'_1 P_1$ in Fig. 9. We assume $\vec{R}_1$ is equal approximately to $\vec{R}$ because displacements of the piezoelectric actuators are very small, less than 0.2 mm. However, half the length of electromagnet, r, is more than 20 mm.

$$\vec{R}_1 = -\vec{R}_2 \approx \frac{r\theta}{\sqrt{2}}\begin{pmatrix}-1\\1\end{pmatrix} = \vec{R} \qquad (1)$$

$$\overrightarrow{O_1P_1} = \begin{pmatrix}x_1\\y_1\end{pmatrix} = \vec{L} + \vec{R}_1 \qquad (2)$$

$$\overrightarrow{O_2P_2} = \begin{pmatrix}x_2\\y_2\end{pmatrix} = \vec{L} + \vec{R}_2 \qquad (3)$$

In Fig. 8, we find the following relationships. Here, we rewrite x_{G1} and y_{G1} as x_G and y_G for simplicity.

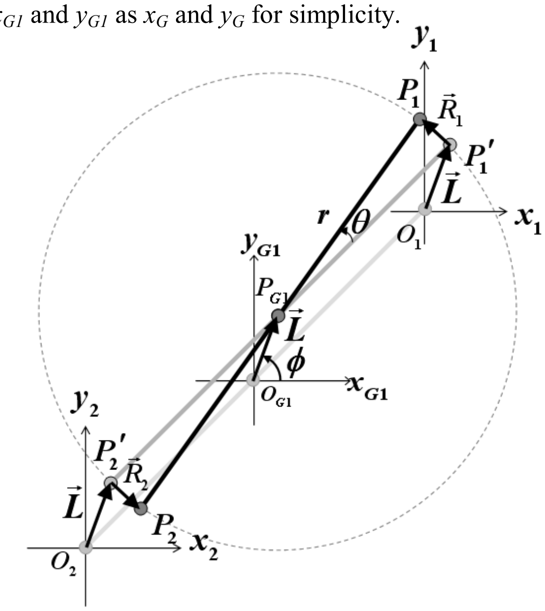

Fig. 8. Vector resolution of EM_1 in X, Y and θ axes

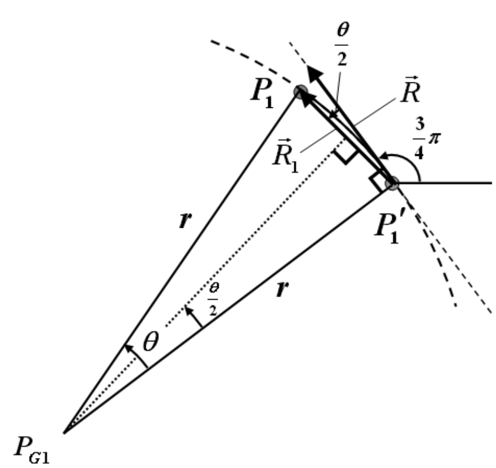

Fig. 9. Geometric analysis of triangle $P_{G1}P'_1 P_1$

$$\overrightarrow{O_G P_G} = \begin{pmatrix} x_G \\ y_G \end{pmatrix} = \frac{1}{2}\begin{pmatrix} x_1 + x_2 \\ y_1 + y_2 \end{pmatrix} = \frac{1}{2}\left(\overrightarrow{O_1 P}_1 + \overrightarrow{O_2 P}_2\right) = \vec{L} \quad (4)$$

When we use the approximation of (1) and (4), we can simplify equations (2), (3) as follows:

$$\overrightarrow{O_1 P}_1 = \begin{pmatrix} x_1 \\ y_1 \end{pmatrix} \approx \begin{pmatrix} x_G \\ y_G \end{pmatrix} + \frac{r\theta}{\sqrt{2}}\begin{pmatrix} -1 \\ 1 \end{pmatrix} \quad (5)$$

$$\overrightarrow{O_2 P}_2 = \begin{pmatrix} x_2 \\ y_2 \end{pmatrix} \approx \begin{pmatrix} x_G \\ y_G \end{pmatrix} - \frac{r\theta}{\sqrt{2}}\begin{pmatrix} -1 \\ 1 \end{pmatrix} \quad (6)$$

We find an important relationship among x_1, y_1, x_2, and y_2 as shown in the equation (7).

$$x_1 - x_2 + y_1 - y_2 \approx 0 \quad (7)$$

This equation means that EM_1 is a rigid body. The mechanism has 3 DOF and the input parameters are 4 input voltages of the piezoelectric actuators. Equation (7) represents one condition. In Fig. 7, force of point P_1 is

$$\vec{F}_1 = \begin{pmatrix} F_{1x} \\ F_{1y} \end{pmatrix} = -k_S\begin{pmatrix} x_1 \\ y_1 \end{pmatrix} + k_L\begin{pmatrix} d_F - x_1 \\ d_R - y_1 \end{pmatrix}. \quad (8)$$

Force of point P_2 is

$$\vec{F}_2 = \begin{pmatrix} F_{2x} \\ F_{2y} \end{pmatrix} = -k_S\begin{pmatrix} x_2 \\ y_2 \end{pmatrix} + k_L\begin{pmatrix} -d_B - x_2 \\ -d_L - y_2 \end{pmatrix}. \quad (9)$$

Newton's second low of translational motion of EM_1 is calculated as below,

$$m\begin{pmatrix} \ddot{x}_G \\ \ddot{y}_G \end{pmatrix} = \vec{F}_1 + \vec{F}_2 = -2\left(k_S + k_L\right)\begin{pmatrix} x_G \\ y_G \end{pmatrix} + k_L\begin{pmatrix} d_F - d_B \\ d_R - d_L \end{pmatrix}. \quad (10)$$

We define displacements of piezoelectric actuators as the following:

$$\begin{cases} d_F = A_F \sin\omega t + l_0 \\ d_B = A_B \sin\omega t + l_0 \\ d_R = A_R \sin\omega t + l_0 \\ d_L = A_L \sin\omega t + l_0 \end{cases} \quad (11)$$

l_0 is the offset displacement. As explained in Fig. 5, A_F is the amplitude displacement of PZT_F. A_B, and A_R, and A_L is similarly defined. When we substitute (11) into (10), we obtain linear differential equations of x_G and y_G.

$$\ddot{x}_G + \frac{2\left(k_S + k_L\right)}{m} x_G = \frac{k_L\left(A_F - A_B\right)}{m}\sin\omega t \quad (12)$$

$$\ddot{y}_G + \frac{2\left(k_S + k_L\right)}{m} y_G = \frac{k_L\left(A_R - A_L\right)}{m}\sin\omega t \quad (13)$$

Newton's second law of the rotational motion of EM_1 is calculated as below,

$$I_G\ddot{\theta} = \frac{r}{\sqrt{2}}\begin{pmatrix} 1 \\ 1 \end{pmatrix} \times \vec{F}_1 + \frac{r}{\sqrt{2}}\begin{pmatrix} -1 \\ -1 \end{pmatrix} \times \vec{F}_2,$$

$$I_G\ddot{\theta} = \frac{r}{\sqrt{2}}\{k_L\left(A_R + A_L - A_F - A_B\right)\sin\omega t + \left(k_S + k_L\right)\left(x_1 - x_2 - y_1 + y_2\right)\}. \quad (14)$$

Here, I_G is the inertia moment of EM_1 around the center of mass. From (1), (2), and (3),

$$\vec{P}_1 - \vec{P}_2 = \begin{pmatrix} x_1 - x_2 \\ y_1 - y_2 \end{pmatrix} = 2\vec{R}_1 \approx 2\vec{R} = \sqrt{2}r\theta\begin{pmatrix} -1 \\ 1 \end{pmatrix},$$

$$x_1 - x_2 - \left(y_1 - y_2\right) \approx -2\sqrt{2}r\theta. \cdots\cdots (15)$$

When we substitute (15) into (14), we obtain linear differential equations of θ,

$$\ddot{\theta} + \frac{2r^2\left(k_S + k_L\right)}{I_G}\theta = \frac{rk_L\left(A_R + A_L - A_F - A_B\right)}{\sqrt{2}I_G}\sin\omega t. \quad (16)$$

We define the initial conditions as follows:

$$x_G(0) = \dot{x}_G(0) = y_G(0) = \dot{y}_G(0) = \theta(0) = \dot{\theta}(0) = 0 \quad (17)$$

The solutions to the differential equations of (12), (13) and (16) become the following:

$$x_G = \frac{A_F - A_B}{2} \cdot \frac{\omega_{nL}^2}{-\omega^2 + \omega_n^2}\left(\sin\omega t - \frac{\omega}{\omega_n}\sin\omega_n t\right) \quad (18)$$

$$y_G = \frac{A_R - A_L}{2} \cdot \frac{\omega_{nL}^2}{-\omega^2 + \omega_n^2}\left(\sin\omega t - \frac{\omega}{\omega_n}\sin\omega_n t\right) \quad (19)$$

$$\theta = \frac{A_R + A_L - A_F - A_B}{2\sqrt{2}r} \cdot \frac{\omega_{nRL}^2}{-\omega^2 + \omega_{nR}^2}\left(\sin\omega t - \frac{\omega}{\omega_{nR}}\sin\omega_{nR} t\right) \quad (20)$$

$$\omega_n = \sqrt{\frac{2\left(k_L + k_S\right)}{m}} \quad (21)$$

$$\omega_{nR} = r\sqrt{\frac{2\left(k_L + k_S\right)}{I_G}} \quad (22)$$

$$\omega_{nL} = \sqrt{\frac{2k_L}{m}} \quad (23)$$

$$\omega_{nRL} = r\sqrt{\frac{2k_L}{I_G}} \quad (24)$$

Here, (21) is the natural angular frequency in the vibration of X and Y axes and (22) is the natural angular frequency in rotational vibration around the gravity point. (23) and (24) are the natural angular frequency when shearing forces do not exist.

C. Approximation of oscillations

When we control the mechanism with angular frequency, which is much smaller than natural angular frequency, as in (21) and (22), we can describe (18), (19) and (20) approximately as follows:

$$x_G \approx \frac{A_F - A_B}{2} \cdot \frac{k_L}{k_L + k_S - 2\pi^2 f^2 m}\sin\omega t \quad (25)$$

$$y_G \approx \frac{A_R - A_L}{2} \cdot \frac{k_L}{k_L + k_S - 2\pi^2 f^2 m}\sin\omega t \quad (26)$$

$$\theta \approx \frac{A_R + A_L - A_F - A_B}{2\sqrt{2}r} \cdot \frac{k_L}{k_L + k_S - 2\pi^2 f^2 \frac{I_G}{r^2}}\sin\omega t \quad (27)$$

D. Step width and step angle

As depicted in Fig. 5, we switch magnetic force at every peak of the sine wave. We design the 1 step motion to be mainly determined by peak-to-peak amplitudes of piezoelectric displacements, $2A_F$, $2A_B$, $2A_R$ and $2A_L$. However, we need to consider the influence of k_L, k_S, f and m from (25), (26) and (27), when shearing forces are not negligible and driving frequency and mass are increased. Peak-to-peak amplitudes of x_G, (25), and y_G, (26), make a step width, W.

$$W = \frac{k_L}{k_L + k_S - 2\pi^2 f^2 m}\sqrt{\left(A_F - A_B\right)^2 + \left(A_R - A_L\right)^2} \qquad (28)$$

We determine the maximum and minimum value of displacement amplitudes as follows:

$$-l_0 \le A_F, A_B, A_R, A_L \le l_0 \qquad (29)$$

As depicted in Figs. 7 and 8, when EM_1 moves to a plus y_G direction, $\phi = \pi/2$, with maximum step width, the combination of amplitudes become as follows:

$$A_F = 0,\ A_B = 0,\ A_R = l_0,\ A_L = -l_0 \qquad (30)$$

We see that the mechanism keeps moving to the plus y_G direction when it repeats its inchworm motion as in Fig. 5. A substitution of (30) to (28) results in the maximum step width of orthogonal motion, $W_{ortho.}$. Here, we assume orthogonal motion is straight motion in $\phi = 0, \pi/2, \pi, 3\pi/2$.

$$W_{ortho.} = \frac{2k_L l_0}{k_L + k_S - 2\pi^2 f^2 m} \qquad (31)$$

A substitution of (30) to (27) confirms that this motion is translational motion because θ is zero. When EM_1 moves to diagonally forward left in a straight line, $\phi = 3\pi/4$, with maximum step width, the combination of amplitudes become as follows:

$$A_F = -l_0,\ A_B = l_0,\ A_R = l_0,\ A_L = -l_0 \qquad (32)$$

Using the same procedure, we get maximum step width of diagonal straight motions, $\phi = \pi/4, 3\pi/4, 5\pi/4, 7\pi/4$.

$$W_{diago.} = \sqrt{2}\frac{2k_L l_0}{k_L + k_S - 2\pi^2 f^2 m}\left(= \sqrt{2} \cdot W_{ortho.}\right) \qquad (33)$$

We use these simplified equations to calculate the required performance of piezoelectric actuators and electromagnets for accurate inchworm motion. In this paper, we focus on orthogonal motions, $\phi = 0, \pi/2, \pi, 3\pi/2$ and $\theta = 0$, to calculate the required performance of piezoelectric actuators and electromagnets.

IV. Calculation of Maximum Velocity with No Slip

A. Maximum frequency with no slip

The purpose of this paper is the analysis of the maximum velocity with good repeatability. We assume that a slip of electromagnets influences motion repeatability. Frictional force between fixed electromagnet, EM_2, and floor surface should be more than the inertia force of EM_1, $F_{inertia}$, when there is no slip. The following conditions must be satisfied when μ is a coefficient of static friction.

$$F_{inertia} \le \mu F_{mag} \qquad (36)$$

$F_{inertia}$ with W_{ortho} is calculated from (25), (26), (30) and (31).

$$F_{inertia} = m\sqrt{\ddot{x}_G^2 + \ddot{y}_G^2} \le \frac{2k_L l_0\left(2\pi^2 f^2 m\right)}{k_L + k_S - \left(2\pi^2 f^2 m\right)} = m\left(2\pi f\right)^2 \cdot \frac{W_{ortho.}}{2} \qquad (37)$$

When we substitute (37) into (36), we get maximum frequency, $f_{inertia\text{-}max}$, with no slip.

$$f \le f_{inertia-max} = \frac{1}{\pi}\sqrt{\frac{\mu F_{mag}\left(k_L + k_S\right)}{2m\left(2k_L l_0 + \mu F_{mag}\right)}} \qquad (38)$$

We should consider the slip of magnets when frequency, f, becomes more than $f_{inertia\text{-}max}$. The current rise time, τ and the magnetic force, F_{mag}, are mainly determined by the voltage and current source of its amplifier. In this paper, we use the amplifier with a voltage source of 12 V and a current source of 0.35 A. As shown in table II, τ of "C" is about 0.4 ms and that of "G" is 2.5 ms. The F_{mag} of "C" is about 4 N and that of "G" is 8 N at 0.35 A. The mass of the electromagnet of "C" is 13.5 g and that of "G" is 20.3 g. From (38) and table II, we get the $f_{inertia\text{-}max}$ of "G ", which is 177.4 Hz and that of "C", which is 378.7 Hz as shown in table II. We consider another limitation of maximum frequency, $f_{rise\text{-}max}$, made from current rise time as shown below:

$$f_{rise-max} = \frac{1}{2\tau} \qquad (39)$$

If the frequency becomes more than (39), electromagnets can not generate the maximum magnetic force. The $f_{rise\text{-}max}$ of "C" is 1250 Hz and that of "G" is 667 Hz. Because $f_{rise\text{-}max}$ is more than $f_{inertia\text{-}max}$, we assume that maximum frequencies with no slip become $f_{inertia\text{-}max}$.

B. Maximum velocity with no slip

If there is no slip, the velocity of translational motion, V, is mainly determined as follows:

$$V \approx W \times f \qquad (40)$$

We assume that there are f steps in a unit of time and the step width, W, is a constant value at all steps. We get the maximum velocity of orthogonal motions, $V_{ortho.}$, when we substitute (31) into (40).

$$V_{ortho.} \approx \frac{2k_L l_0 f}{k_L + k_S - 2\pi^2 f^2 m} \qquad (41)$$

When we substitute (38) into (41), we get maximum velocity, $V_{ortho.\text{-}max}$, of orthogonal motions.

$$V_{ortho.-max} = \frac{1}{\sqrt{2}\pi} \times \sqrt{\mu\frac{F_{mag\_max}}{m}} \times \sqrt{\frac{2l_0 \cdot k_L + \mu F_{mag\_max}}{k_L + k_S}} \qquad (42)$$

The $V_{ortho.\text{-}max}$ of "G" becomes 18.3 mm/s and that of "C" becomes 7.9 mm/s from (42). Table II shows the quantities used for the calculations. We determine k_S and μ from other

TABLE II
QUANTITIES FOR CALCULATIONS

Symbol	Quantity	C type	G type
F_{mag}	Electromagnetic Force [N]	4.0	8.0
τ	Current rise time [ms]	0.15	2.5
m	Mass of an electromagnet [g]	13.5	20.3
$2\pi\omega_n$	Natural Frequency [Hz]	1575.6	550.4
$f_{inertia\text{-}max}$	Maximum frequency (no slip) [Hz]	**378.7**	**177.4**
$f_{rise\text{-}max}$	Maximum frequency (rise time) [Hz]	1250	667
$V_{ortho.\text{-}max}$	Maximum velocity (no slip) [mm/s]	**7.9**	**18.3**
μ	Coefficient of static friction	0.2	0.2
l_0	Amplitude displacement [μm]	16.2(100V)	60(120V)
k_s	Spring constant of shearing force [N/m]	367,500	34,500
k_l	Spring constant of PZT[N/m]	490,000	115,000
	Height-Width-Length [mm]	20-30-30	23-50-50
	Weight [g]	37.1	65.9

experiments. From (42), we designed electromagnets to increase the ratio of magnetic force to mass. We also reduced the spring constant of shear conversion, k_S. The more we increase l_0, the less the spring constant k_L becomes. That is because the piezoelectric actuator amplifies displacement of stacked type piezoelectric element by the mechanical amplifier. If k_L becomes smaller, the natural angular frequency also becomes smaller from (21). If the natural angular frequency becomes too small, the term of $-\omega/\omega_n \sin\omega_n t$ in (18) and (19) can not negligible. This term works as a disturbance when we want to keep step width constant with every step. If the step width changes with every step, the moving distance is not proportional to the number of steps and operability becomes worse. In this paper, we assume that the natural frequency is more than 500 Hz when we move "G" type less than 200 Hz. From table II, we see that "G" is designed to increase l_0 and to decrease natural frequency as much as possible. The positioning resolution of "G" is larger than that of "C" because we amplify displacement of PZT. However, we confirmed "G" still has less than 100 nm resolution.

V. Experimental Results

As shown in Fig. 10, we measure the mechanism's position by an image analyzer and a CCD-camera with 4 million pixels. We put LEDs, as measuring points, on the mechanism. The measuring accuracy is about 10 μm. Surface roughness is about R_{ms} 0.2 μm. We generate input signals by DA board (Labview PCI-6723) and amplify 30-fold by the amplifier. We measure path length of 100 steps every 50 Hz. Then we calculate the average step width and velocity at each frequency. As shown in Figs. 11 and 12, we have confirmed that the experimental step width and velocity are consistent with the theoretical values up to $f_{inertia\text{-}max}$. We also confirmed that the newly developed "G" has over twice the maximum velocity of "C". When frequency is more than $f_{inertia\text{-}max}$, the difference between experimental and theoretical values increases because of the slip. These experimental results indicate that we can increase the velocity if we use the slip of electromagnets positively as skating motion.

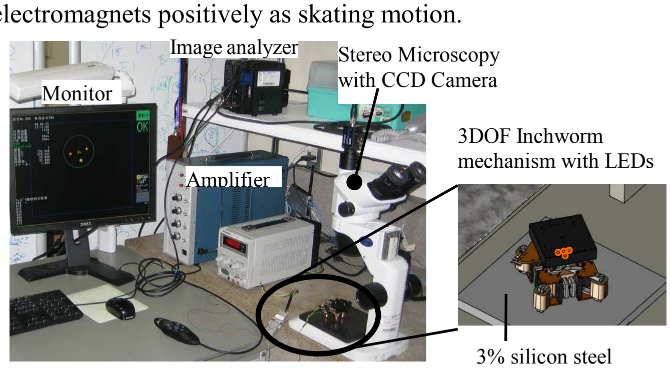

Fig. 10. Experimental setup

VI. Conclusion and Future Work

We have described dynamical analysis for the 3 DOF precise inchworm mechanism. Experimental results show that the proposed analysis is effective in estimating the velocity with no slip condition. We have also succeeded in increasing the maximum velocity over 2 times compared with a conventional mechanism. We have also developed the high-speed positioning devices for chip mounting application for this mechanism. For future work, we plan to measure motion repeatability and durability. We also plan to develop the slip-based motion to improve the maximum velocity for long distance navigation.

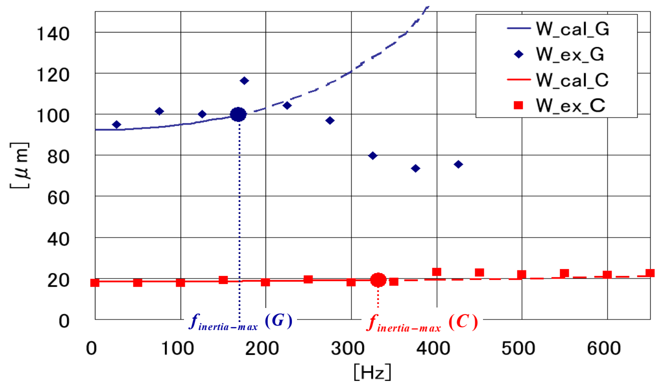

Fig. 11. Relationship between step width and frequency

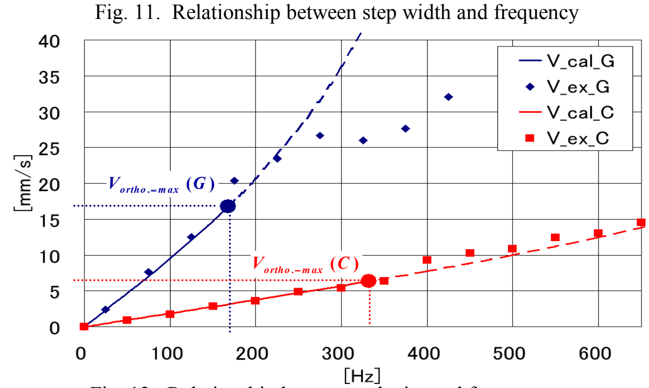

Fig. 12. Relationship between velocity and frequency

References

[1] O. Fuchiwaki, A. Ito, D. Misaki and H. Aoyama: Multi-axial Micromanipulation Organized by Versatile Micro Robots and Micro Tweezers, Proc. of IEEE Int. Conference on Robotics & Automation(ICRA2008), pp.893-898, 2008

[2] O. Fuchiwaki, D. Misaki, C. Kanamori and H. Aoyama: Development of the Orthogonal Micro Robot for Accurate Microscopic Operations, Journal of Micro-Nano Mechatronics (JMNM) , Vol.4, No.1-2, pp.85-93, 2008

[3] S. Martel, M. Sherwood, C. Helm, W.G. de Quevedo, "Three-legged wireless miniature robots for mass-scale operations at the sub-atomic scale", Proc. of 2001 ICRA. IEEE International Conference on Volume 4, pp.3423-3428, 2001

[4] W. Driesen, T. Varidel, S. Regnier, J-M Breguet, "Micro manipulation by adhesion with two collaborating mobile micro robots", Journal of Micromechatronics and Microengineering, 15, S259-S267, 2005

[5] J. M. Brequet, W. Driesen, F. Kaegi, T. Cimprich: Applications of piezo-actuated micro-robots in micro-biology and material science, Proc. of the 2007 IEEE International Conference on Mechatronics and Automation, pp.57-62, 2007

[6] S. Fatikow, et al.: Automated Nanohandling by microrobots, Springer series in advanced manufacturing, Springer, ISBN 978-1-84628-977-4, 2008

[7] O. Fuchiwaki, T. Kawai, A. Ohta, D. Misaki and H. Aoyama: Development of a Positioning & Compensation Device for a Versatile Micro Robot, Proc. of IEEE Int. Conference on Intelligent Robots and Systems (IROS 2008), pp.83-88, September, 22nd to 26th, Niece, France, 2008